P. Sudhrasana Rao, C. Nagakotareddy / International Journal of Engineering Research and Applications (IJERA) ISSN: 2248-9622 www.ijera.com
Vol. 3, Issue 4, Jul-Aug 2013, pp.1996-2001

An Enhanced ZVS & ZCS Full Bridge Converter With Resonance Circuit In The Secondary Winding For High Power Applications

P. Sudhrasana Rao[1], C. Nagakotareddy[2]
[1]Assistant Professor, Dept. of EEE, NIE College, Macherla,
[2] P.G.Student Dept. of EEE, NIE College, Macherla.

ABSTRACT

A zero voltage and zero current switching full bridge converters with a resonance circuit in the secondary winding is presented analyzed. The primary side of the converter is composed of FB insulated-gate bipolar transistors, which are driven by phase-shift control. The secondary side is composed of a resonant tank and a half-wave rectifier. Without an auxiliary circuit, zero-voltage switching (for leading-leg switches) and zero-current switching (for lagging-leg switches) are achieved in the entire operating range. To implement the converter without an additional inductor, the leakage inductance of the transformer is utilized as the resonant inductor. Due to its many advantages, including high efficiency, minimum number of devices, and low cost, this converter is attractive for high-voltage and high-power applications. The analysis and design considerations of the converter are presented. A prototype was implemented for an application requiring a 5-kW output power, an input-voltage range varying from 250 to 350 V, and a 350-V output voltage. The experimental results obtained from a prototype verify the analysis. The prototype's efficiency at full load is over 95.5%.

I. INTRODUCTION

IN high-frequency and high-power converters, it is desirable to use insulated-gate bipolar transistors (IGBTs) for primary switches and to utilize soft-switching techniques such as zero voltage switching (ZVS) and zero-current switching (ZCS). IGBTs can handle higher voltage and higher power with lower cost compared with MOSFETs, so IGBTs have been Replacing MOSFETs in applications requiring several or several tens of kilowatt power. In high-frequency converters, soft-switching techniques are widely used to reduce the switching loss that results from high switching frequency.

Among previous soft-switching FB converters, a series-resonant converter (SRC) is the simplest topology. Moreover, because all switches of the converter are turned on at zero voltage, the conversion efficiency is relatively high. However, the SRC has some drawbacks. First, the output voltage cannot be regulated for the no-load case. Second, it has some difficulties, such as size reduction and a design of an electromagnetic-interference noise filter because a wide variation of the switching frequency is necessary to control the output voltage.

Some modified converters based on a conventional SRC have been presented to solve these problems. One is a converter that utilizes other control methods without additional hardware. By using a control method in, regulation problems under low-power conditions can be solved, but the range of the operating frequency is still wide. Another presented approach is the phase-shift control of SRC, such as the ZVS FB converters in and The ZVS FB converters can achieve constant-frequency operation, no regulation problem, and ZVS of all switches that are composed of MOSFETs. Because all switches of the converters are MOSFETs, the converters are not adequate for high-power conversion in the power range of several or tens of kilowatts. To apply the converter for high-power conversions, further improvements, such as applying IGBTs and extending the soft-switching range, are necessary.

The proposed converter has several advantages over existing converters. First, the leading-leg switches can be turned on softly under almost all operating conditions, and a lossless turn-off snubber can be used to reduce turn-off loss. Second, the lagging-leg switches can be turned on at zero voltage and also turned off near zero current without additional auxiliary circuits. Third, the reverse-recovery currents of the diodes are significantly reduced, and the voltage stresses of the output diodes are clamped to the output voltage. Therefore, last, the switching loss of the converter is very low, and the converter is adequate for high-voltage and high-power applications.

II. PRINCIPAL OF OPERATION

The operation of the converter in Fig. 1 is analyzed in this section. The output voltage V_o of the converter is controlled as in a conventional phase-shifted FB converter. The converter has six operation modes within each switching period T_s.

The operation waveforms and equivalent circuits are shown in Figs. 2 and 3, respectively. To analyze the operation of the converter, several assumptions are made in the following.

1) Leading-leg switches T_1 and B_1 and lagging-leg switches T_2 and B_2 are ideal, except for their body diodes.
2) Because the output capacitor C_o is very large, the output voltage V_o is a dc voltage without any ripple.
3) Transformer T is composed of ideal transformers N_1 and N_2, a magnetizing inductance L_m, and a leakage inductance L_{lk}.
4) Since the capacitances of lossless turn-off snubber (CT_1 and CB_1) are very small, the transient time of charging and discharging is neglected.
5) When the switching frequency f_s is less than the resonant frequency f_r, the conduction loss is large unnecessarily due to the high peak currents of the devices. Therefore, we assume that $f_s \geq f_r$.

The voltage across N_2 is given as three-level voltages: nV_{in}, 0, and $-nV_{in}$ by the phase-shift control of the primary switches, where n is the transformer turn ratio N_2/N_1 and Vin is the input voltage. The series-resonant tank is formed by L_{lk} and a resonant capacitor Cr, the secondary current is through the resonant circuit is half-wave rectified by the rectifying diodes D_1 and D_2, and the positive value of is feeds the output stage.

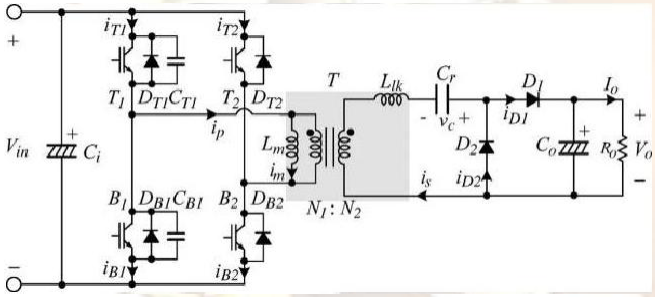

Fig. 1. *Proposed soft-switching FB converter with secondary resonance*

A detailed mode analysis is as follows.

Mode 1 [t_0, t_1]*:* As shown in Figs. 2 and 3, top switches T_1 and T_2 are ON state, and is becomes zero at t_0. During this mode, diodes D_1 and D_2 are OFF state, and the current is remains zero. Because the voltages across both N_1 and N_2 are zero, the magnetizing current im is constant. The following equalities are satisfied.

$$i_m(t) = i_p(t) = i_{T1}(t) = -i_{T2}(t) = i_m(t_2) \quad (1)$$

Where i_p is the primary current and i_{T1} is the sum of the currents of T_1, its body diodes DT_1's, and its snubber capacitance C_{T1}. Similarly, i_{T2}, i_{B1}, and i_{B2} are defined. The currents of body diodes are simply the negative portions of i_{T1}, i_{T2}, i_{B1}, and i_{B2}.

Mode 2 [t_1, t_2]*:* At t_1, the lagging-leg switch T_2 is turned off when $iT_2 = -i_m$. Because i_m is a very low current, T_2 is turned off near zero current. After a short dead time, B_2 is turned on at zero voltage, while the current ip flows through the body diode of B_2. During this mode, the secondary voltage across N_2 is nV_{in}. Therefore, i_s builds up from its zero value and flows through $D1$. The state equations can be written as follows:

$$L_{lk}\frac{di_s(t)}{dt} + V_0 - v_c(t) = nV_{in}$$
$$C_r\frac{d(V_0 - v_c(t))}{dt} = i_s(t)$$
$$i_s(t) = 0 \quad (2)$$

Where v_c is a voltage across Cr. Thus, i_s is obtained as

$$i_s(t) = \frac{(nV_{in} - (V_o - V_c(t_1))}{z_o}\sin\omega_r(t-t_1) \quad (3)$$

Where the angular resonance frequency

$$\omega_r = 2\Pi f_r = \frac{1}{\sqrt{L_{lk}C_r}} \quad (4)$$

and the characteristic impedance

$$Z_0 = \sqrt{\frac{L_r}{C_r}} \quad (5)$$

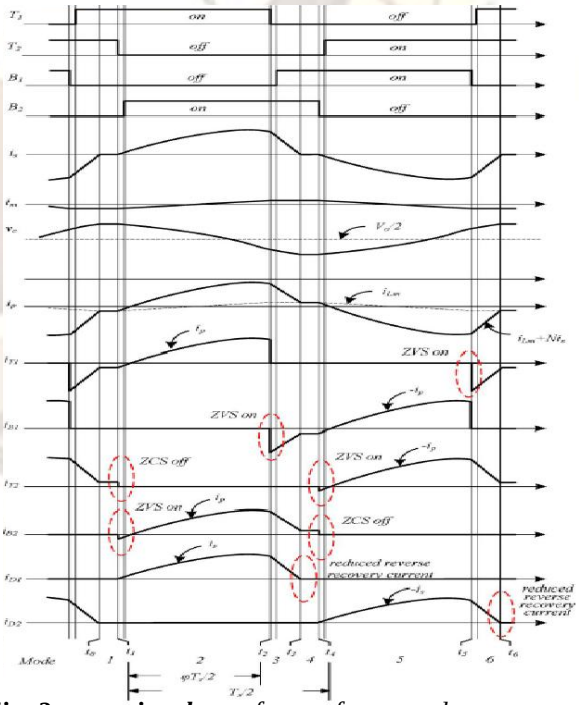

Fig: 2: operational *waveforms of proposed converter*

The magnetizing current i_m is increased linearly by the input voltage as

$$i_m(t) = i_m(t_1) + \frac{V_{in}}{L_m}(t - t_1) \quad (6)$$

The following equalities are also satisfied:

$$i_p(t) = i_m(t) = ni_s(t) = i_{T1}(t) = i_{B2}(t) \quad (7)$$

Mode 3 [t_2, t_3]: At t_2, T_1 is turned off

.Subsequently, the current i_p charges CT_1 and discharges CB_1. Once the collector–emitter voltage of B_1 reaches zero, the current *ip* flows through the body diode of B_1. After dead time, B_1 is turned on at zero voltage. Because the voltage across N_2 is zero, *is* goes to zero. The state equation is the same as (2), except for the initial condition of *is* and the applied voltage across N_2.Thus, the current *is* can be obtained analogously with (3) as

$$i_s(t) = i_s(t_2)\cos\omega_r(t-t_2) - \frac{V_o - V_c(t_2)}{Z_o}\sin\omega_r(t-t_2) \quad (8)$$

The following equalities are also satisfied:

$$i_p(t) = i_m(t) + ni_s(t) = -i_{B1}(t) + i_{B2}(t) \quad (9)$$

At the end of *Mode 3*, *is* becomes zero. Explanations of *Modes 4–6* are omitted because these modes are similar to *Modes 1–3*, respectively.

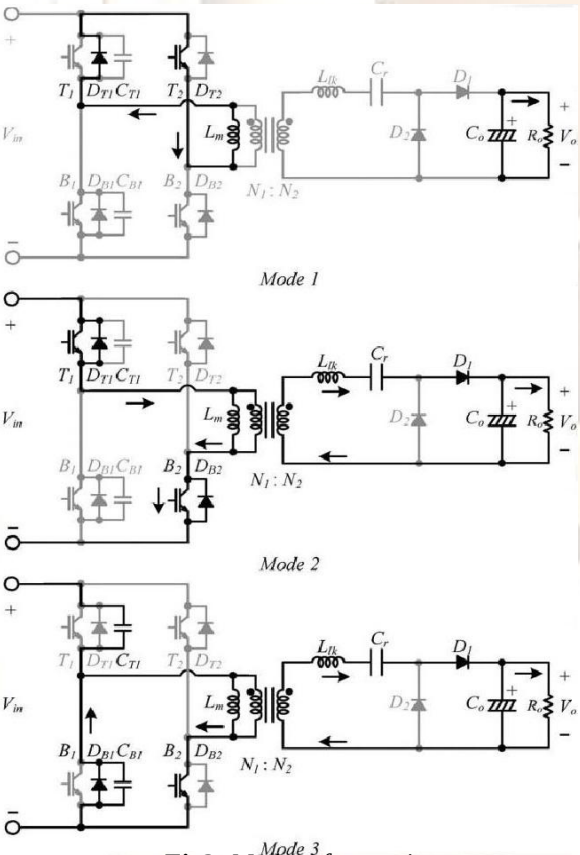

Fig3: *Modes of operation*

The primary current of the conventional ZVS FB converter is compared with the *ip* of the proposed converter (Fig.2).The conventional ZVS FB converter uses a large leakage inductor to achieve the ZVS of the lagging–lag switches in a wide operating range. The large leakage inductor causes higher circulating energy that significantly increases the conduction loss and further reduces the effective duty ratio. On the other hand, in the proposed converter, the effective duty ratio is not reduced, and the conduction loss from the circulating energy is relatively low by resetting the secondary current during *Mode 3*. To analyze the converter, two quantities are defined as frequency ratio

$$F = \frac{f_r}{f_s} \quad (10)$$

and quality factor

$$Q = \frac{4\omega_r L_{lk}}{R_o} \quad (11)$$

III. Analysis of ZVS and ZCS Conditions

In almost the entire operating range, leading-leg switches T_1 and B_1 are naturally turned on at zero voltage by the reflected current *is*, as shown in Fig. 2. However, to achieve ZVS and ZCS in lagging-leg switches T_2 and B_2, *Modes 1* and *4* have to exist, as shown in Fig. 2. In other words, the secondary current must be zero before the switching of T_2 and B_2. Assuming that $F \leq 1$, there are three possible waveforms of the secondary current, as shown in Fig. 5. When the waveform of *is* is similar to Fig. 4(b), the lagging-lag switches cannot be turned off softly at zero current. On the other hand, when the waveform of *is* is similar to Fig. 4(c), T_2 and B_2 cannot be turned on at zero voltage. To achieve the waveform of Fig. 5(a), which is different from that of Fig. 5(b), *is* must reach zero while the secondary voltage across N_2 is zero. Thus, t_3, which satisfies (12), must exist

$$i_m(t_3) = \frac{nV_{in} - (V_o - V_c(t_1))}{Z_o}\sin\omega r(t_3-t_2)\cos\omega_r(t_3-t_2) - \frac{V_o - V_c(t_2)}{Z_o}\sin\omega_r(t_3-t_2) = 0 \quad (12)$$

To achieve the waveform of Fig. 4(a), which is different from that of Fig. 4(c), the peak-to-peak value of the ripple voltage of *Cr* must be lower than V_o. In other words, $vc(t_1)$, which is the minimum value of *vc*, must be positive to avoid the conduction of D_2 during *Mode 4*.

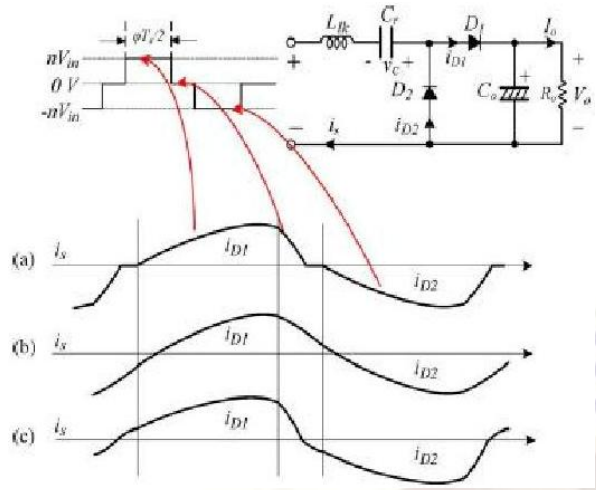

Fig. 4: *Three possible waveforms of the secondary current is. (a) Waveform of is when IGBTs can be turned on and off softly. (b) Waveform of is when IGBTs cannot be turned off softly. (c) Waveform of is when IGBTs cannot be turned on softly.*

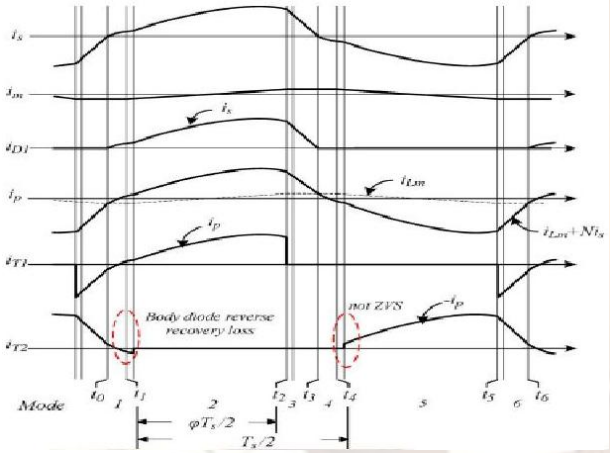

Fig. 5: *Operation waveforms when Q is greater than 2/πF.*

Therefore, from (12), the following inequality must be satisfied:

$$V_o=V_c(t_1)=\frac{V_o}{2}(1-\frac{\pi}{2}FQ) >0 \qquad (13)$$

Therefore, the ZVS condition of T_2 and B_2 is obtained as

$$Q<\frac{2}{\Pi F} \qquad (14)$$

In practical situations, Q may become greater than $2/\pi F$ under overload conditions. Fig. 7 shows the operation waveforms when $Q > 2/\pi F$. Because ZVS cannot be achieved in the lagging-leg switches, switching loss results from the body-diode reverse-recovery current and the dissipated energy of the parasitic output capacitances, as shown in Fig. 7.

However, in IGBTs, the loss resulting from non-ZVS is not large. In real switches, there are parasitic output capacitances C_{oss}'s. Therefore, another ZVS condition of the lagging-leg switches is that the energy stored in *Lm* before T_2 and B_2 are turned on must be greater than the energy stored in the C_{oss} of T_2 and B_2 as

$$\frac{1}{2}L_m\left(\frac{\Delta i_m}{2}\right) > C_{oss}V^2_{in} \qquad (15)$$

Where

$$\Delta i_m=\frac{\emptyset v_{in}}{2L_m f_s} \qquad (16)$$

Therefore, *Lm* can be determined as

$$L_m < \frac{\emptyset^2_{min}}{32C_{oss}f_s^2} \qquad (17)$$

Where ϕ_{min} is the minimum value of ϕ satisfying the ZVS of T_2 and B_2. Another condition of the ZVS of the lagging-lag switches is that the dead time of the lagging leg should be short enough since the lagging-leg switches should be turned on while the current flows through the body diodes. The dead time can simply be determined by experiment.

IV. SIMULATION RESULTS

A prototype of the proposed converter was simulated through matlab. The converter was tested with *Vin* = 250 V, *Vo* = 550 V, and output power *Po* = 1.3 kW; further design parameters are given in Table I.

TABLE 1: Simulation Parameters

PERAMETERS	SYMBOL	VALUE
Input voltage range	Vin	250V
Output voltage	V0	550V
Output power	P0	1.3KW
Magnetizing inductance	Lm	300µH
Leakage inductance	Llk	15.7µH
Quality factor at rated condition	Q	0.62
Resonant frequency	f_r	38.3kHz
Switching frequency	f_s	38.3kHz
Resonant capacitor	C_r	1.1µF
Snubber capacitor	CT1,CB1	6.8nF

Fig: 6(a) & (b) shows the zero voltage and zero current i.e. soft switching waveforms of the leading leg and lagging leg switches.

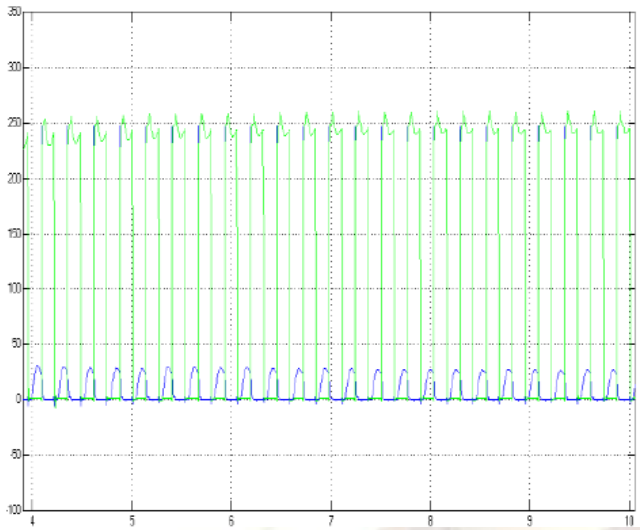

Fig: 6(a) *soft switching waveforms of leading leg switches*

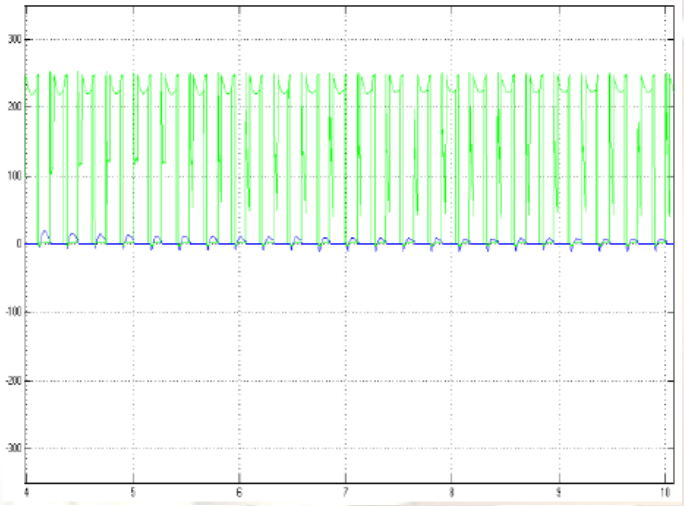

Fig: 6(b) *soft switching waveforms of lagging leg switches*

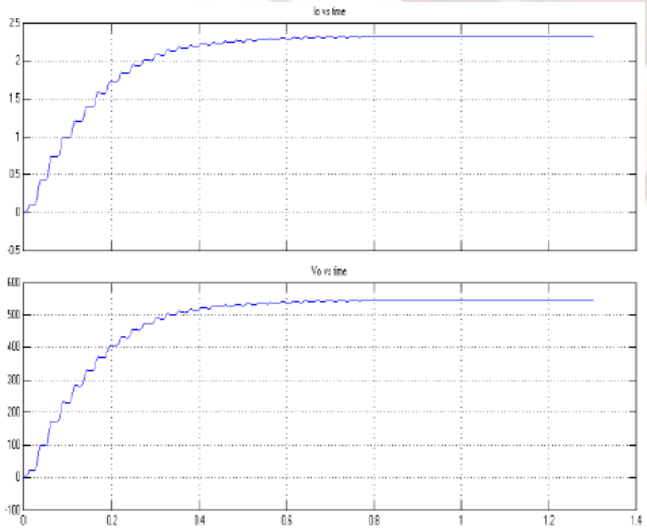

Fig7: *output voltage and current waveforms*

V. CONCLUSION

The operation of the proposed converter is analyzed. And the experimental results of a 1.2KW prototype prove the novel converter is successful. The efficiency attained under full-load conditions was over 95.5%. The converter may be adequate for high-voltage and high-power applications (> 10 kW) since the converter has many advantages, such as minimum number of devices, soft switching of the switches, no output inductor, and so on.

REFERENCES

[1] X. Wu, J. Zhang, X. Ye, and Z. Qian,―Analysis and derivations for a family ZVS converter based on a new active clamp ZVS cell,‖ *IEEE Trans. Ind. Electron.*, vol. 55, no. 2, pp. 773–781, Feb. 2008.

[2] J. J. Lee, J. M. Kwon, E. H. Kim, and B. H. Kwon, ―Dual series resonant active-clamp converter,‖ *IEEE Trans. Ind. Electron.*, vol. 55, no. 2, pp. 699–710, Feb. 2008.

[3] B. R. Lin and C. H. Tseng, ―Analysis of parallel-connected asymmetrical soft-switching converter,‖ *IEEE Trans. Ind. Electron.*, vol. 54, no. 3, pp. 1642–1653, Jun. 2007.

[4] C. M. Wang, ―A novel ZCS-PWM fly back converter with a simple ZCSPWM commutation cell,‖ *IEEE Trans. Ind. Electron.*, vol. 55, no. 2, pp. 749–757, Feb. 2008.

[5] P. Das and G. Moschopoulos, ―A comparative study of zero-current transition PWM converters,‖ *IEEE Trans. Ind. Electron.*, vol. 54, no. 3, pp. 1319–1328, Jun. 2007.

[6] G. C. Jung, H. R. Geun, and F. C. Lee, ―Zero-voltage and zero-current switching full-bridge PWM converter using secondary active clamp,‖ in *Proc. IEEE PESC*, 1996, vol. 1, pp. 657–663.

[7] J. Zhang, X. Xie, X. Wu, G. Wu, and Z. Qian, ―A novel zero-current transition full bridge DC/DC converter,‖ *IEEE Trans. Power Electron.*, vol. 21, no. 2, pp. 354–360, Mar. 2006.

[8] T. T. Song and N. Huang, ―A novel zero-voltage and zero-current switching full-bridge PWM converter,‖ *IEEE Trans. Power Electron.*, vol. 20, no. 2, pp. 286– 291, Mar. 2005.

[9] E. S. Kim and Y. H. Kim, ―A ZVZCS PWM FB DC/DC converter using a modified energy-recovery snubber,‖ *IEEE Trans. Ind. Electron.*, vol. 49, no. 5, pp. 1120–1127, Oct. 2002.

[10] K. W. Seok and B. H. Kwon, ―An

improved zero-voltage and zerocurrent-switching full-bridge PWM converter using a simple resonantcircuit,‖ *IEEE Trans. Ind. Electron.*, vol. 48, no. 6, pp. 1205–1209, Dec. 2001.

[11] X. Wu, X. Xie, C. Zhao, Z. Qian, and R. Zhao, ―Low voltage and current stress ZVZCS full bridge DC–DC converter using center tapped rectifier reset,‖ *IEEE Trans. Ind. Electron.*, vol. 55, no. 3, pp. 1470–1477, Mar. 2008.

[12] J. Dudrik, P. Spanik, and N. D. Trip, ―Zero-voltage and zero-current switching full-bridge DC–DC converter with auxiliary transformer,‖ *IEEE Trans. Power Electron.*, vol. 21, no. 5, pp. 1328– 1335, Sep. 2006.

[13] X. Wu, X. Xie, C. Zhao, Z. Qian, and R. Zhao, ―Low voltage and current stress ZVZCS full bridge DC–DC converter using center tapped rectifier reset,‖ *IEEE Trans. Ind. Electron.*, vol. 55, no. 3, pp. 1470–1477, Mar. 2008.

[14] R. L. Steigerwald, ―A comparison of half bridge resonant converter topologies, *IEEE Trans. Power Electron.*, vol. 3, no. 2, pp. 174–182, Apr. 1998.

Author Information:

P.Sudharsana Rao was born in Guntur, India. He received the B.Tech (Electronics and Instrumentation Engineering) degree from the Jawaharlal Nehru Technological University, Kakinada in 2010. M.Tech (Control System Engineering) from the IIT Khargpur. He is currently an Asst.Professor of the Dept. of Electrical and Electronic Engineering, Newton's Institute of Engineering, Macherla. His area of interest Biomedical Engineering and Control Systems.

C.Nagakotareddy was born in Prakasam, India. He received the B.Tech (Electrical and Electronics Engineering) degree from The Jawaharlal Nehru Technological University, Kakinada in 2010. Currently pursuing M-Tech (Electrical Machines and Drives), in Newton's Institute of Engineering, Macherla in 2013. His area of interested in Power Electronics applications in Electrical Machines.